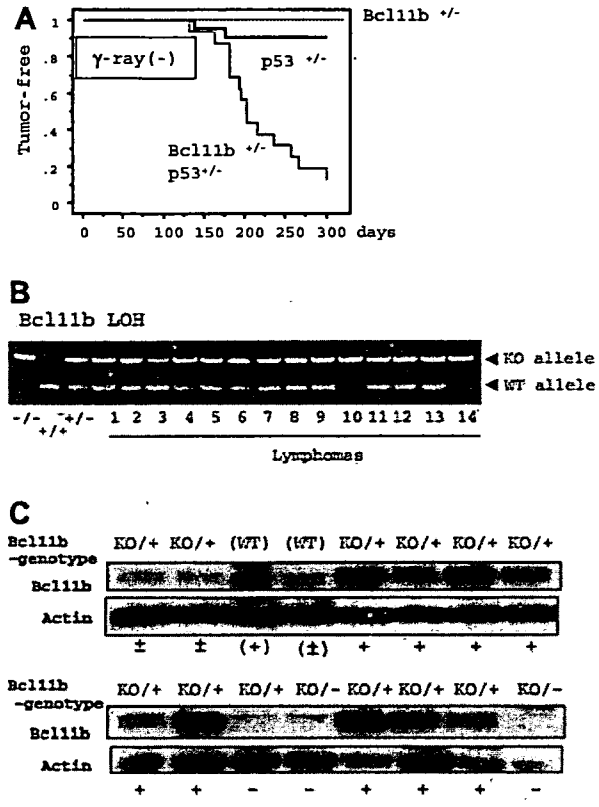

Fig. 2. Haploinsufficiency of the *Bcl11b* gene for tumor suppression. (A) Kaplan–Meier analysis of spontaneously developed thymic lymphomas in $Bcl11b^{+/-}p53^{+/-}$ (gray line), $p53^{+/-}$ (black line) and $Bcl11b^{+/-}$ (dotted line) mice. (B) Loss of heterozygosity analysis. Most lymphomas from $Bcl11b^{+/-}p53^{+/-}$ mice did not show loss of wild-type *Bcl11b* allele (only two of 14 tumors did). (C) Retained expression of Bcl11b proteins in most lymphomas. Nine lymphomas showed strong expression (indicated by +), two moderate expression (+/−), and three (two of them are of KO/− genotype) showed loss of expression (−). WT, two lymphomas from $Bcl11b^{+/+}p53^{+/-}$ mice are also shown.

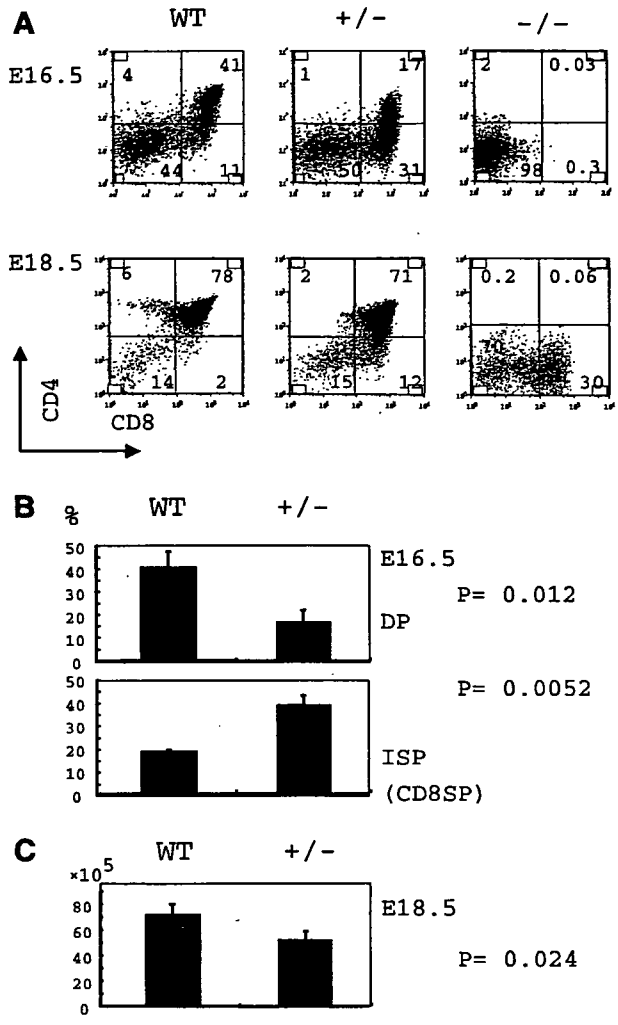

Fig. 3. Haploinsufficiency of *Bcl11b* for thymocyte differentiation. (A) Flowcytometric analysis of thymocytes from $Bcl11b^{+/+}$, $Bcl11b^{+/-}$, and $Bcl11b^{-/-}$ embryo littermates at E16.5 and E18.5. Panels show expression of CD4 and CD8. The percent of cells is shown in the appropriate quadrant. (B,C) Summary of three independent analyses of the flowcytometry. Bars display the percentages of cells in double-positive (DP) and CD8 immature single-positive (ISP) subpopulations in $Bcl11b^{+/+}$ and $Bcl11b^{+/-}$ thymocytes (B). Bars represent the number of viable thymocytes (C). Error lines represent standard deviation. *P* values were obtained by χ^2 test using StatView-J 5.0 software.

as found in *p53* [14] where loss of the two alleles was more tumorigenic than loss of one.

Bcl11b is haploinsufficient for thymocyte differentiation

Study of brain tissues of *Bcl11b* heterozygotes revealed a haploinsufficiency phenotype; reduced levels of Bcl11b limited the ability of corticospinal motor neurons to properly establish and maintain projections to the spinal cord [15]. We therefore examined effect of the *Bcl11b* heterozygosity on thymocyte differentiation at embryonic stages, though our previous examination failed to detect the influence [8]. Approximately, 40% of thymocytes from $Bcl11b^{+/+}$ mice at E16.5 were in the CD4 and CD8 double-positive (DP) fraction whereas only 20% of thymocytes from $Bcl11b^{+/-}$ littermates were in the DP fraction (Fig. 3A and B). $Bcl11b^{+/+}$ mice at E18.5 showed an elevation in the number of thymocytes compared to $Bcl11b^{+/-}$ mice (Fig. 3C). These results indicate that loss of one copy of *Bcl11b* hinders thymocyte differentiation and proliferation at the embryonic stage.

Discussion

This paper shows that $Bcl11b^{+/-}$ mice were more susceptible to thymic lymphomas than $Bcl11b^{+/+}$ mice when irradiated. Without irradiation, $Bcl11b^{+/-}$ genotype also provided the susceptibility in combination with the $p53^{+/-}$ genotype. These results indicate that *Bcl11b* possesses a suppressor function for thymic lymphoma development. In the lymphomas developed in the $Bcl11b^{+/-}p53^{+/-}$ mice, *Bcl11b* heterozygous state contributed to lymphomagenesis even

retaining the expression, indicating that *Bcl11b* is a haploinsufficient tumor suppressor gene. The mechanism of influence to lymphomagenesis of *Bcl11b* heterozygosity in the *p53* heterozygous background is unclear, but not ascribed to acceleration of loss of the wild-type *p53* allele, since 12 of the 14 lymphomas retained the wild-type *p53* allele (data not shown).

The haploinsufficiency could be a more general feature of tumor suppressor genes than previously assumed. These include *p53*, *Pten*, *p27*, *Chk1*, and *Cdc42* [14,16–19]. $Pten^{+/-}p53^{+/-}$ doubly heterozygous mice are more susceptible to tumorigenesis than $Pten^{+/-}$ or $p53^{+/-}$ singly heterozygous mice [16], as seen in $Bcl11b^{+/-}p53^{+/-}$ mice. This suggests synergistic effects of the two genes, *p53* and *Pten*, on tumor development. Interestingly, however, mutual exclusiveness of mutations was observed between *Pten* and *p53*, suggesting that the two molecules are on a common signaling pathway [20,21]. The two findings of synergy and mutual exclusiveness seem to contradict each other and the mechanism for the discrepancy is not yet elucidated. The genetic synergy and the mutual exclusiveness of mutations were also seen for *Bcl11b* and *p53*. Our previous study showed that intragenic deletions in *Bcl11b* were found in *p53* wild-type lymphomas at a much higher frequency than in *p53*-deficient lymphomas [13], although this study demonstrated their synergistic effects on lymphoma development.

Recent studies indicate that the human *BCL11B* locus on chromosome 14q32 is recurrently involved in chromosomal aberrations in hematopoietic malignancies mostly of T-cell origin [10,11]. These aberrations are characterized as DNA rearrangements between *BCL11B* and other chromosomal loci in T-cell acute lymphoblastic leukemias (T-ALL) and acute myelocytic leukemias [22–26]. However, since the majority of T-ALL expressed BCL11B from an undisrupted allele, it was difficult to conclude whether BCL11B acts as a tumor suppressor gene or an oncogene. Our finding that *Bcl11b* is a haploinsufficient tumor suppressor gene strongly suggests that chromosomal disruptions at *BCL11B* in human leukemia/lymphomas contribute to oncogenesis even when BCL11B is expressed from an undisrupted allele.

Acknowledgments

We thank O. Niwa and A. Balmain for helpful comments on the manuscript. This work was supported by Grants-in-Aid for Cancer Research from the Ministries of Education, Science, Art and Sports, and was also supported by Grants-in-Aid for Cancer Research (13-2) from the Ministry of Health, Labor and Welfare of Japan.

References

[1] B. Vogelstein, K.W. Kinzler, The multi-step nature of cancer, Trends Genet 9 (1993) 138–141.
[2] C.J. Sherr, Principles of tumor suppression, Cell 116 (2004) 235–246.
[3] W.D. Cook, B.J. McCaw, Accommodating haploinsufficient tumour suppressor genes in Knudson's model, Oncogene 19 (2004) 3434–3438.
[4] K.C. Quon, A. Berns, Haplo-insufficiency? Let me count the ways, Genes Dev. 15 (2001) 2917–2921.
[5] D. Avram, A. Fields, K. Pretty On Top, D.J. Nevrivy, J.E. Ishmael, M. Leid, Isolation of a novel family of C2H2 zinc finger proteins implicated in transcriptional repression mediated by chicken ovalbumin upstream promoter transcription factor (COUP-TF) orphan nuclear receptors, J. Biol. Chem. 275 (2000) 10315–10322.
[6] E. Satterwhite, T. Sonoki, T.G. Willis, L. Harder, R. Nowak, E.L. Arriola, H. Liu, H.P. Price, S. Gesk, D. Steinemann, B. Schlegelberger, D.G. Oscier, R. Siebert, P.W. Tucker, M.J. Dyer, The BCL11 gene family: involvement of BCL11A in lymphoid malignancies, Blood 98 (2001) 3413–3420.
[7] Y. Wakabayashi, H. Watanabe, J. Inoue, N. Takeda, J. Sakata, Y. Mishima, J. Hitomi, T. Yamamoto, M. Utsuyama, O. Niwa, S. Aizawa, R. Kominami, Homozygous deletions and point mutations of the Rit1/Bcl11b gene in γ-ray induced mouse thymic lymphomas, Biochem. Biophys. Res. Commun. 301 (2003) 598–603.
[8] Y. Wakabayashi, H. Watanabe, J. Inoue, N. Takeda, J. Sakata, Y. Mishima, J. Hitomi, T. Yamamoto, M. Utsuyama, O. Niwa, S. Aizawa, R. Kominami, Bcl11b is required for differentiation and survival of αβ T lymphocytes, Nat. Immunol. 4 (2003) 533–539.
[9] J. Inoue, T. Kanefuji, K. Okazuka, H. Watanabe, Y. Mishima, R. Kominami, Expression of TCRαβ partly rescues developmental arrest and apoptosis of αβT cells in $Bcl11b^{-/-}$ mice, J. Immunol. 176 (2006) 5871–5879.
[10] V. Bezrookove, S.L. van Zelderen-Bhola, A. Brink, K. Szuhai, A.K. Raap, R. Barge, G.C. Beverstock, C. Rosenberg, A novel t(6;14)(q25–q27;q32) in acute myelocytic leukemia involves the BCL11B gene, Cancer Genet. Cytogenet. 149 (2004) 72–76.
[11] G.K. Przybylski, W.A. Dik, J. Wanzeck, P. Grabarczyk, S. Majunke, J.I. Martin-Subero, R. Siebert, G. Dolken, W.D. Ludwig, B. Verhaaf, J.J. van Dongen, C.A. Schmidt, A.W. Langerak, Disruption of the BCL11B gene through inv(14)(q11.2q32.31) results in the expression of BCL11B-TRDC fusion transcripts and is associated with the absence of wild-type BCL11B transcripts in T-ALL, Leukemia 19 (2005) 201–208.
[12] Y. Matsumoto, S. Kosugi, T. Shinbo, D. Chou, M. Ohashi, Y. Wakabayashi, K. Sakai, M. Okumoto, N. Mori, S. Aizawa, O. Niwa, R. Kominami, Allelic loss analysis of gamma-ray-induced mouse thymic lymphomas: two candidate tumor suppressor gene loci on chromosomes 12 and 16, Oncogene 16 (1998) 2747–2754.
[13] J. Sakata, J. Inoue, H. Ohi, H. Kosugi-Okano, Y. Mishima, K. Hatakeyama, O. Niwa, R. Kominami, Involvement of V(D)J recombinase in the generation of intragenic deletions in the Rit1/Bcl11b tumor suppressor gene in γ-ray-induced thymic lymphomas and in normal thymus of the mouse, Carcinogenesis 25 (2004) 1069–1075.
[14] S. Venkatachalam, Y.P. Shi, S.N. Jones, H. Vogel, A. Bradley, D. Pinkel, L.A. Donehower, Retention of wild-type p53 in tumors from p53 heterozygous mice: reduction of p53 dosage can promote cancer formation, EMBO J. 17 (1998) 4657–4667.
[15] P. Arlotta, B.J. Molyneaux, J. Chen, J. Inoue, R. Kominami, J.D. Macklis, Neuronal subtype-specific genes that control corticospinal motor neuron development in vivo, Neuron 45 (2005) 207–221.
[16] D.J. Freeman, A.G. Li, G. Wei, H.H. Li, N. Kertesz, R. Lesche, A.D. Whale, H. Martinez-Diaz, N. Rozengurt, R.D. Cardiff, X. Liu, H. Wu, PTEN tumor suppressor regulates p53 protein levels and activity through phosphatase-dependent and -independent mechanisms, Cancer Cell 3 (2003) 117–130.
[17] M.L. Fero, E. Randel, K.E. Gurley, J.M. Roberts, C.J. Kemp, The murine gene $p27^{Kip1}$ is haplo-insufficient for tumor suppression, Nature 396 (1998) 177–180.
[18] M.H. Lam, Q. Liu, S.J. Elledge, J.M. Rosen, Chk1 is haploinsufficient for multiple functions critical to tumor suppression, Cancer Cell 6 (2004) 45–59.

[19] J.H. Mao, J. Perez-Losada, D. Wu, R. Delrosario, R. Tsunematsu, K.I. Nakayama, K. Brown, S. Bryson, A. Balmain, Fbxw7/Cdc4 is a p53-dependent, haploinsufficient tumour suppressor gene, Nature 432 (2004) 775–779.

[20] H. Kato, S. Kato, T. Kumabe, Y. Sonoda, T. Yoshimoto, S. Kato, S.Y. Han, T. Suzuki, H. Shibata, R. Kanamaru, C. Ishioka, Functional evaluation of p53 and PTEN gene mutations in gliomas, Clin. Cancer Res. 6 (2000) 3937–3943.

[21] K. Kurose, K. Gilley, S. Matsumoto, P.H. Watson, X.P. Zhou, C. Eng, Frequent somatic mutations in PTEN and TP53 are mutually exclusive in the stroma of breast carcinomas, Nat. Genet. 32 (2002) 355–357.

[22] O.A. Bernard, M. Busson-LeConiat, P. Ballerini, M. Mauchauffe, V. Della Valle, R. Monni, F. Nguyen Khac, T. Mercher, V. Penard-Lacronique, P. Pasturaud, L. Gressin, R. Heilig, M.T. Daniel, M. Lessard, R. Berger, A new recurrent and specific cryptic translocation, t(5;14)(q35;q32), is associated with expression of the Hox11L2 gene in T acute lymphoblastic leukemia, Leukemia 15 (2001) 1495–1504.

[23] T. Itoyama, R.S. Chaganti, Y. Yamada, K. Tsukasaki, S. Atogami, H. Nakamura, M. Tomonaga, K. Ohshima, M. Kikuchi, N. Sadamori, Cytogenetic analysis and clinical significance in adult T-cell leukemia/lymphoma: a study of 50 cases from the human T-cell leukemia virus type-1 endemic area, Nagasaki, Blood 97 (2001) 3612–3620.

[24] R.A. MacLeod, S. Nagel, M. Kaufmann, J.W. Janssen, H.G. Drexler, Activation of HOX11L2 by juxtaposition with 3′-BCL11B in an acute lymphoblastic leukemia cell line (HPB-ALL) with t(5;14)(q35;q32.2), Genes Chromosomes Cancer 37 (2003) 84–91.

[25] S. Nagel, M. Kaufmann, H.G. Drexler, R.A. MacLeod, The cardiac homeobox gene NKX2-5 is deregulated by juxtaposition with BCL11B in pediatric T-ALL cell lines via a novel t(5;14)(q35.1;q32.2), Cancer Res. 63 (2003) 5329–5334.

[26] X. Su, H. Drabkin, E. Clappier, E. Morgado, M. Busson, S. Romana, J. Soulier, R. Berger, O.A. Bernard, C. Lavau, Transforming potential of the T-cell acute lymphoblastic leukemia-associated homeobox genes HOXA13, TLX1, and TLX3, Genes Chromosomes Cancer 45 (2006) 846–855.

doi:10.1111/j.1440-1746.2006.03373.x

CASE REPORT

Liver injury induced by a Japanese herbal medicine, sairei-to (TJ-114, Bupleurum and Hoelen Combination, Chai-Ling-Tang) R1

Tsuneo Aiba,* Toru Takahashi,* Kenji Suzuki,* Shogo Okoshi,* Minoru Nomoto,* Katsuji Uno† and Yutaka Aoyagi*

*Division of Gastroenterology and Hepatology, Graduate School of Medical and Dental Sciences, Niigata University, and †Department of Pharmacy, Suibarago Hospital, Niigata, Japan

Key words
hepatitis, herbal medicine, liver, sairei-to (Bupleurum and Hoelen Combination, Chai-Ling-Tang).

Accepted for publication 6 October 2003.

Correspondence
Dr Toru Takahashi, Division of Gastroenterology and Hepatology, Nagaoka Red Cross Hospital, 297-1, Terashimacho, Nagaoka 940-2085, Niigata, Japan.
Email: torutoru@nagaoka.jrc.or.jp

Abstract

The case is reported of a man who showed acute hepatitis with jaundice after he was given a Japanese herbal medicine, sairei-to (TJ-114, Bupleurum and Hoelen Combination, Chai-Ling-Tang). Unusually, the component thought to be responsible for the observed drug-induced liver injury was able to be identified. Lymphocyte migration inhibition testing indicated that the tuber of the perennial herbage *Pinellia ternate* was the causative agent.

Introduction

There is a growing body of evidence that herbal medicine can eventually cause liver injury; nevertheless, it is widely believed to be 'natural', mild-acting and non-toxic. Here we report the case of a man who showed acute hepatitis with jaundice after he was given a Japanese herbal medicine, sairei-to.

Case report

A 37-year-old man visited the Division of Gynecology and Obstetrics, Niigata University Medical Hospital, for the treatment of male infertility. He was prescribed an oral daily dose of the Japanese herbal medicine 'sairei-to' (TJ-114, Bupleurum and Hoelen Combination, Chai-Ling-Tang). He felt easy fatigability 4 weeks later, and noticed his eyeballs were yellowish 7 weeks later. His body temperature was 37.2°C. Eight weeks after commencing sairei-to he returned to the hospital, where liver dysfunction was detected and hence he was referred to our division and immediately admitted to our hepatobiliary unit.

On admission, his consciousness level was alert. No flapping tremor was noted. His bulbar conjunctiva was markedly icteric. Slight tenderness existed at the right hypochondric region and his enlarged liver was palpable by one finger-breadth on the right midclavicular line. Aspartate aminotransferase (AST) and alanine aminotransferase (ALT) levels were markedly elevated at 1816 IU/L and 3660 IU/L, respectively. Total bilirubin was 12.3 mg/dL, and prothrombin time was slightly elongated at 69%. Tests for hepatitis virus markers (including hepatitis A, B, and C), cytomegalovirus and Epstein–Barr virus were not indicative of active viral infection. Although eosinophilia was not present in peripheral blood (0.5%), sairei-to was suspected to be causative of his liver dysfunction. Thus, discontinuation of sairei-to was indicated.

Lymphocyte migration inhibition test (LMIT) was carried out initially for sairei-to, and then for 11 herbal components that comprise sairei-to. Sairei-to as a whole was found to evoke a positive LMIT reaction. Among the 11 herbal components, both hange (*Pinellia* tuber) and chorei (*Polyporus umbellatus*, chulling, Zhu Ling Tang) were positive. As chorei evoked a positive LMIT reaction even in a control test, hange was finally determined to be a most probable causative component in this drug-induced liver injury.

Discontinuation of the drug, and bed rest with drip infusion of electrolyte-containing fluid was indicated to the patient. From that point, ALT and lactate dehydrogenase (LDH) levels gradually reduced towards the normal range (Fig. 1). Jaundice initially became worse, reached a plateau and then gradually resolved. The peak value of total bilirubin was 23.4 mg/dL. About a month later, liver function tests returned to nearly normal.

Liver biopsy was performed on the 33rd hospital day under his full informed consent. Hepatic lobular architecture was preserved with slightly enlarged portal tracts with fibrosis. Focal necroses were scattered throughout hepatic lobules. In hepatic sinusoids, mild eosinophilic infiltration was seen. In portal tracts, macrophages that imbibed bile pigments were focally accumulated. Eosinophils were also scattered among other types of infiltrating cells

Journal of Gastroenterology and Hepatology 22 (2007) 762–763

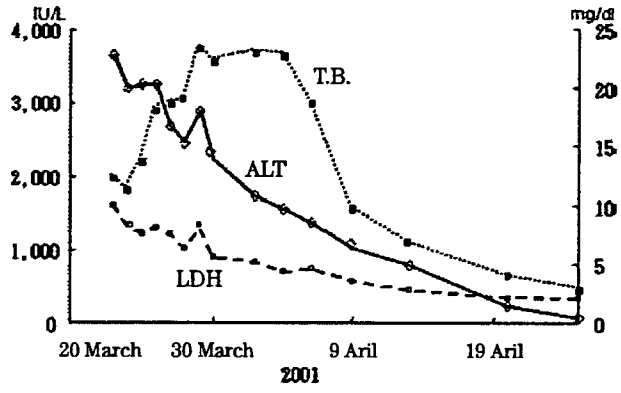

Figure 1 Clinical course of the patient over time. ALT, alanine aminotransferase; LDH, lactate dehydrogenase; TB, total bilirubin.

in slightly enlarged portal tracts. Tissue eosinophilia in the liver biopsy specimen strongly suggested an allergic nature of this acute hepatitis.

The patient was discharged from our hospital on the 35th hospital day without any further disease sequelae.

Discussion

Among various modalities of alternative medicine, Chinese herbal medicine is most prevalent world-wide. Herbal medicine is not only given by medical facilities but also sold over the counter by herbal medicine venders in the community. As the amount of herbal medicines consumed increased, more reports appeared concerning untoward effects including liver injuries putatively caused by herbal medicines. These include acute hepatitis, chronic hepatitis, cholestatic hepatitis, and bile duct injuries.[1] Wild germander (*Teucrium chamaedrys*),[2] syo-saiko-to (TJ-9, Xiao-Chai-Hu-Tang),[3] cascara sagrada[4] and dai-saiko-to (TJ-8, Da-Chai-Hu-Tang)[5] are reported to cause various drug-induced liver injuries.

A regular herbal medicine usually consists of several herbal components as well as some ingredients that cannot be excluded in the process of purification. Therefore, it is important to determine what herbal component or ingredient is mainly responsible for the observed liver injury whenever the herbal medicine as a whole shows a positive reaction in lymphocyte sensitivity assay. In this context, our report seems to be unique in the point that it demonstrated one herbal component in the standard Chinese herbal medicine to be responsible for the observed drug-induced liver injury by means of LMTT. The responsible herbal component in sairei-to, 'hange' or pinellia tuber in English, consists of the tuber of the perennial herbage *Pinellia ternate* breit. Thus, the single compound in the tuber that essentially caused liver injury has to be further elucidated.

References

1 Chitturi S, Farrell GC. Herbal hepatotoxicity: an expanding but poorly defined problem. *J. Gastroenterol. Hepatol.* 2000; 15: 1093–9.
2 Larrey D, Vial T, Pauwels A *et al.* Hepatitis after germander (*Teucrium chamaedrys*) administration: another instance of herbal medicine hepatotoxicity. *Ann. Intern. Med.* 1992; 117: 129–32.
3 Itoh S, Marutani K, Nishijima T, Matsuo S, Itabashi M. Liver injuries induced by herbal medicine, syo-saiko-to (xiao-chai-hu-tang). *Dig. Dis. Sci.* 1995; 40: 1845–8.
4 Nadir A, Reddy D, Van Thiel DH. *Cascara sagrada*-induced intrahepatic cholestasis causing portal hypertension: case report and review of herbal hepatotoxicity. *Am. J. Gastroenterol.* 2000; 95: 3634–7.
5 Kamiyama T, Nouchi T, Kojima S, Murata N, Ikeda T, Sato C. Autoimmune hepatitis triggered by administration of an herbal medicine. *Am. J. Gastroenterol.* 1997; 92: 703–4.

Pathology International 2007; **57**: 413–420 doi:10.1111/j.1440-1827.2007.02117.x

Original Article

Blockade of interferon-γ-inducible protein-10 attenuates chronic experimental colitis by blocking cellular trafficking and protecting intestinal epithelial cells

Kenji Suzuki,[1] Yusuke Kawauchi,[1] Suresh S. Palaniyandi,[2] Punniyakoti T. Veeraveedu,[2] Masato Fujii,[3] Satoshi Yamagiwa,[1] Hiroyuki Yoneyama,[4] Gi Dong Han,[5,6] Hiroshi Kawachi,[5] Yoshiaki Okada,[6] Yoichi Ajioka,[7] Kenichi Watanabe,[2] Masamichi Hosono,[3] Hitoshi Asakura,[1] Yutaka Aoyagi[1] and Shosaku Narumi[4]

Departments of [1]Gastroenterology and Hepatology, [5]Cell Biology, Institute of Nephrology and [7]Pathology, Niigata University Graduate School of Medical and Dental Sciences, [2]Department of Clinical Pharmacology, Niigata University of Pharmacy and Applied Life Sciences, [3]Department of Life Science, Niigata University Graduate School of Science and Technology, Niigata City, [4]Stelic Institute and [6]Department of Bacterial and Blood Products, National Institute of Infectious Diseases, Tokyo, Japan and [8]Department of Food Science and Technology, Yeungnam University, Gyeongsan, Korea

The role of chemokines, especially CXCL10/interferon-γ-inducible protein 10 kDa (IP-10), a chemokine to attract CXCR3⁺ T-helper 1-type CD4⁺ T cells, is largely unknown in the pathophysiology of inflammatory bowel disease; ulcerative colitis and Crohn's disease. The authors have earlier shown that IP-10 neutralization protected mice from acute colitis by protecting crypt epithelial cells of the colon. To investigate the therapeutic effect of neutralization of IP-10 on chronic colitis, an anti-IP-10 antibody was injected into mice with newly established murine AIDS (MAIDS) colitis. Anti-IP-10 antibody treatment reduced the number of colon infiltrating cells when compared to those mice given a control antibody. The treatment made the length of the crypt of the colon greater than control antibody. The number of Ki67⁺ proliferating epithelial cells was increased by the anti-IP-10 antibody treatment. Terminal deoxynucleotidyl transferase-mediated dUTP nick-end labeling (TUNEL)⁺ apoptotic cells were observed in the epithelial cells of the luminal tops of crypts in control MAIDS colitis, whereas TUNEL⁺ apoptotic epithelial cells were rarely observed with anti-IP-10 antibody treatment. In conclusion, blockade of IP-10 attenuated MAIDS colitis through blocking cellular trafficking and protecting intestinal epithelial cells, suggesting that IP-10 plays a key role in the development of inflammatory bowel disease as well as in chronic experimental colitis.

Correspondence: Kenji Suzuki, MD, PhD, Department of Gastroenterology and Hepatology, Niigata University Graduate School of Medical and Dental Sciences, 1-757 Asahimachi-dori, Niigata 951-8510, Japan. Email: kjsuzuki@med.niigata-u.ac.jp

Received 3 October 2006. Accepted for publication 20 February 2007.

Key words: epithelial hyperplasia, IP-10, murine AIDS, ulcerative colitis

Chemokines, which are chemotactic cytokines, control the essential process of the attraction of leukocytes to tissues in inflammation.[1,2] The chemokine family consists of two major subfamilies, termed CXC and CC according to the arrangement of the first two conserved cysteines that are separated by one amino acid and are adjacent, respectively.[1,2] The interferon (IFN)-γ-inducible protein of 10 kDa (IP-10/CXCL10) is a member of the CXC chemokine family, and a potent chemoattractant for activated T lymphocytes, natural killer (NK) cells, and monocytes.[3,4] It is also considered as a regulator of the T-helper 1 (Th1) inflammatory response.[5] It has been reported that the expression of IP-10 was elevated in several diseases such as ulcerative colitis, hepatitis, multiple sclerosis, and Sjögren's syndrome, suggesting the involvement of IP-10 in the development of these diseases.[6–9] Information on the role of IP-10 in inflammatory bowel disease is limited, and needs further detailed investigation.

We have recently reported that neutralization of IP-10 protected mice from dextran sulfate sodium (DSS)-induced acute colitis by promoting crypt cell survival, without altering the infiltration of immune cells.[10] Furthermore, recombinant IP-10 administration into mice directly inhibited the intestinal epithelial cell proliferation.[10] In contrast, another report showed that IP-10 neutralization dominantly inhibited inflammation, and ameliorated colitis in interleukin-10 (IL-10)-deficient mice.[11] Thus, the therapeutic mechanism of IP-10 neutralization on experimental colitis has yet to be shown clearly.

The LP-BM5 murine leukemia virus (MuLV) is a retrovirus that induces profound immunodeficiency similar to that of human acquired immunodeficiency syndrome (AIDS), therefore it has been studied as a murine model of AIDS, thus termed murine AIDS (MAIDS).[12–15] We have previously reported that systemic exocrinopathy resembling Sjögren's syndrome and pancreatitis-like lesions were induced in mice with MAIDS, and colitis was not induced in MAIDS mice.[16,17] In contrast, nude mice inoculated with lymph node cells from mice with MAIDS developed chronic inflammatory bowel disease-like colitis, which we termed MAIDS colitis.[18] The precise mechanism of pathogenesis of the colitis remains largely unknown, however, regulatory T cells (Treg) deficiency might play a role in its development because there are some reports of colitis modulated by Treg.[19,20] We demonstrated that the pathological lesions of MAIDS colitis resembled ulcerative colitis, and that the major populations of colon-infiltrating cells in MAIDS colitis were $Mac1^+$ macrophages and $CD4^+$ T cells with polarized immune responses toward Th2.[21] Thus, MAIDS colitis could serve as an animal model for ulcerative colitis.

There have been other colitis models developed including DSS colitis, IL-10-deficient mice, and $Rag2^{-/-}$ mice reconstituted with $CD4^+CD45RB^{high}$ T cells, which are characterized as a Th1-dependent disease, mimicking Crohn's disease.[22] The diversity in the etiopathophysiology of these colitis models might induce different effects with IP-10 blockade. Therefore, to confirm the therapeutic mechanism of IP-10 neutralization, it is better to analyze the effect of anti-IP-10 treatment in different type of colitis models. In this report, to address this point, we investigated the effect of IP-10 neutralization on MAIDS colitis.

MATERIALS AND METHODS

Animals

Four-week-old female C57BL/6 (B6) mice were purchased from Charles River Japan (Atsugi, Japan). B6 nude mice were provided by Dr Norimitsu Satoh at the Animal Center of Niigata University School of Medicine. All mice were maintained at the same animal center under specific pathogen-free conditions. All animal experiments were performed according to the Guide for Animal Experimentation of Niigata University School of Medicine.

Induction of MAIDS and MAIDS colitis

Four-week-old B6 female mice were injected i.p. with 0.3 mL LP-BM5 MuLV stock solution. Induction of MAIDS was confirmed when the mice developed generalized lymphadenopathy. Eight weeks after virus inoculation, mice with MAIDS were killed by cervical dislocation under ether anesthesia, and their all lymph nodes were collected. To induce MAIDS colitis, the lymph nodes were pressed and passed through a steel mesh, and the cell suspension was transferred i.v. to 10–13-week-old female B6 nude mice at a dose of $3–5 \times 10^7$ lymph node cells/head. Symptoms of colitis such as diarrhea and anal bleeding were observed 3 weeks after cell transfer, and all the mice died within 6 weeks after cell transfer. LP-BM5 MuLV was prepared from the supernatant of cloned G6 cells infected with the retrovirus as reported previously.[16] For blocking experiments, PBS containing 100 μg/100 μL anti-CXCL10 mAb[10] or antihuman parathyroid-related peptide mAb, which was the IgG1 subclass-matched control mAb, or PBS alone were administered i.p. at the time of cell transfer and once a week thereafter. Three weeks after cell transfer, the mice were killed and their colons were removed for further analysis. Five mice were analyzed for each group and all the experiments were repeated three times.

Histopathological examination

Tissue samples were taken from the sigmoid colon, fixed in 10% buffered formalin, and then embedded in paraffin wax blocks. Four μm-thick sections were made in the usual way and stained with HE. The stained sections were then examined by light microscopy.

The entire colon (5 mice/group) was sampled. We analyzed the distal colon tissue section located approximately 10 mm from the anal verge to calculate the mean number of infiltrating cells of five different points in the lamina propria of the colon in a high-power field (×400) under a microscope. The crypt length of the colon of each mouse was also calculated as a mean value of five different crypts.

Preparation and flow cytometric analysis of cells that infiltrated the colon

Mouse colonic mucosal mononuclear cells were prepared as follows. Lamina propria mononuclear cells were isolated from the colon at 3 weeks after the induction of colitis as described here. Briefly, the entire colon was opened longitudinally, washed with PBS, and cut into small pieces. The pieces were then incubated with Ca^{2+}- and Mg^{2+}-free Hank's balanced salt solution (HBSS) containing 2.5% fetal bovine serum (FBS) and 1 mmol dithiothreitol (DTT) (Sigma-Aldrich, St Louis, MO, USA) for 30 min to remove mucus and then serially incubated twice in Ca^{2+}- and Mg^{2+}-free HBSS containing 2.5% FBS and 0.75 mmol EDTA (Sigma-Aldrich) for 1 h each. The supernatants from these incubations were collected, pooled, and treated with 1 mg/mL collagenase

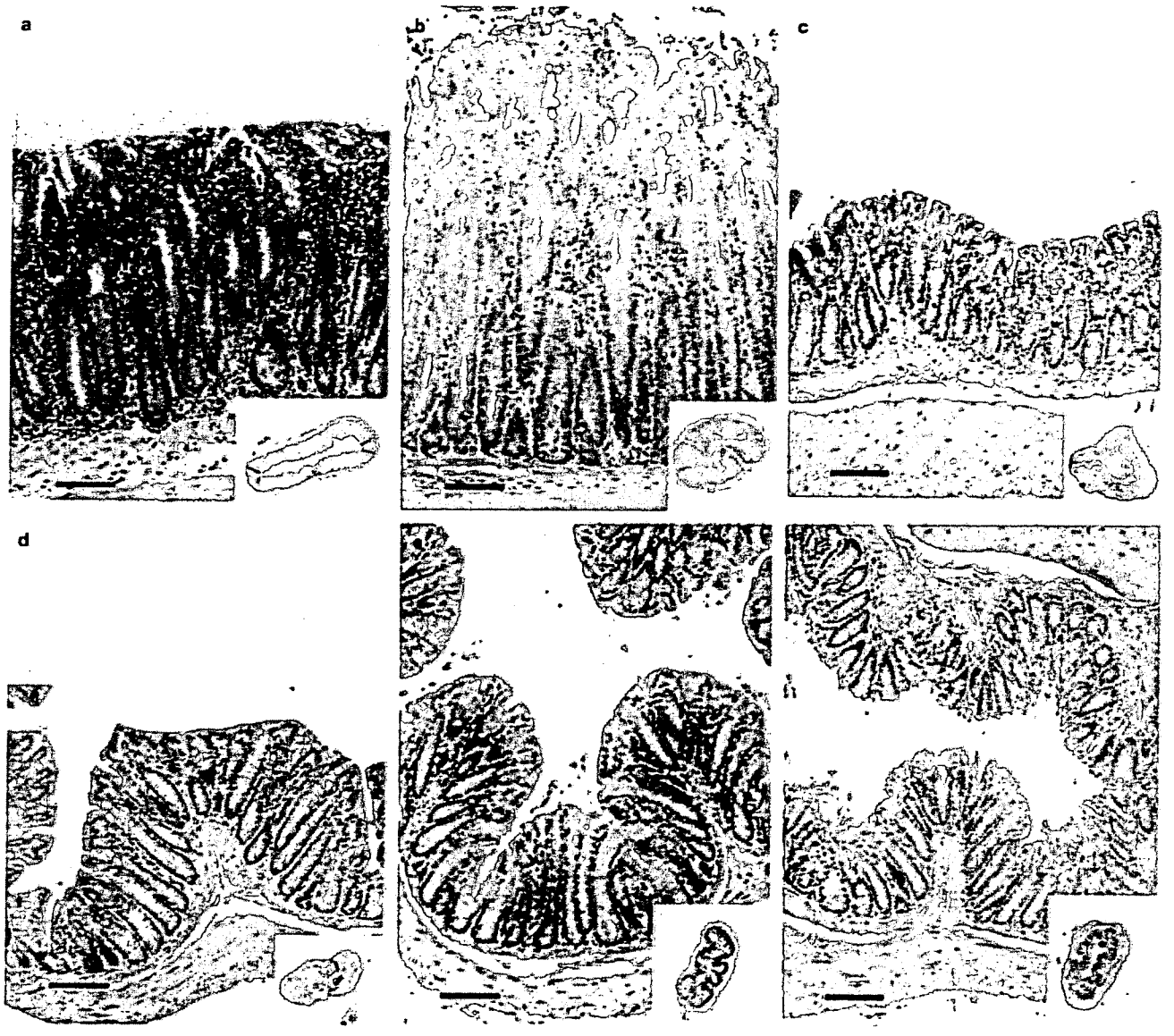

Figure 1 (a–d) Neutralization of interferon-γ-inducible protein 10 kDa (IP-10/CXCL10) attenuated murine acquired immunodeficiency syndrome (MAIDS) colitis. Distal colon tissues: (a) control antibody-treated mouse at 3 weeks after induction of colitis, (b) anti-IP-10 antibody-treated mouse, (c) normal B6 nude mouse, (d) normal B6 mouse, (e) anti-IP-10 antibody-treated B6 nude mouse, (f) anti-IP-10 antibody-treated B6 mouse. (a) Mild erosions of crypt epithelial cells at the tip of the crypt, and crypt abscess were observed in the MAIDS colitis. HE, original magnification ×100. Bars, 100 μm.

(Worthington Biomedical, Freehold, NJ, USA) and 0.01% Dnase (Worthington Biomedical) in medium for 2 h. The cells were pelleted twice through a 40% isotonic Percoll solution (Amersham Pharmacia Biotech AB, Uppsala, Sweden) and then further purified by Ficoll-Hypaque (Pharmacia, Inc., Pisataway, NJ, USA) density gradient centrifugation (40/75%) at 1300 *g*.

Cell suspensions were prepared in PBS containing 1% fetal calf serum and 0.1% sodium azide. The cells were incubated with anti-Fc receptor mAb (2.4G2) for 10 min at 4°C, and then incubated with fluorescent isothiocyanate (FITC)-conjugated mAb and phycoerythrin-conjugated mAb for 30 min. The stained cells were washed twice, resuspended, and analyzed using FACScan (Becton-Dickinson, Mountain View, CA, USA).

Immunohistochemical staining for Ki67

To evaluate the number of proliferating crypt epithelial cells of the colon, we used rabbit polyclonal anti-Ki67 antibody (YLEM, Rome, Italy). Formalin-fixed and paraffin-embedded

colon sections were deparaffinized with xylene and ethanol, and then incubated with the first antibody. FITC-labeled anti-rabbit sheep antibody was then reacted as a secondary antibody. The number of $Ki67^+$ crypt epithelial cells was evaluated under high-power fields on immunofluorescence microscopy.

Terminal deoxynucleotidyl transferase-mediated dUTP nick-end labeling

Apoptotic cells were identified using an *in situ* apoptosis-detection kit (Takara Biomedicals, Otsu, Japan) according to the manufacturer's instructions. In brief, paraffin-embedded colon sections were deparaffinized, rehydrated and then incubated with terminal deoxynucleotidyl transferase mixture containing FITC-dUTP for 90 min at 37°C. After mounting, terminal deoxynucleotidyl transferase-mediated dUTP nick-end labeling $(TUNEL)^+$ cells were counted in a crypt at five different points in high-power fields (×400) on fluorescent microscopy.

Statistical analysis

Data are expressed as mean ± SD. The unpaired Student's *t*-test or the non-parametric Mann–Whitney test was used for statistical analysis. Differences were considered significant at $P < 0.05$.

RESULTS

IP-10 neutralization attenuated MAIDS colitis

In mice treated with control antibody, a marked mononuclear cellular infiltration was observed in the mucosal and submucosal layer at 3 weeks after the induction of colitis (Fig. 1a) in comparison to normal B6 (Fig. 1c) or nude mice (Fig. 1d). Mild erosions of crypt epithelial cells were observed at the tip of crypt, and crypt abscess was also observed in some crypts (Fig. 1a). The number of infiltrating cells in the colon increased gradually with colon weight, and the crypt length significantly increased in MAIDS colitis with control antibody compared to untreated B6 or nude mice (Fig. 2). To evaluate the effect of IP-10 neutralization, we have analyzed the lesions of MAIDS colitis at 3 weeks after the induction of colitis (Fig. 1b). Because a long-term anti-IP-10 antibody treatment induced immunodeficiency and opportunistic infection such as pulmonary abscess at 6 weeks, we therefore carried out the analysis at 3 weeks after the induction of colitis. Neutralization of IP-10 decreased cellular infiltration into the colon of mice with MAIDS colitis (Fig. 2a). In addition, the length of the crypt became significantly greater by IP-10 blockade compared to control MAIDS colitis (Fig. 2b). Neutralization of IP-10 did not produce any significant change either in the number of cells in the lamina propria of the colon or in the length of the crypt of the colon in B6 nude or B6 mice (Figs 1e,f,2).

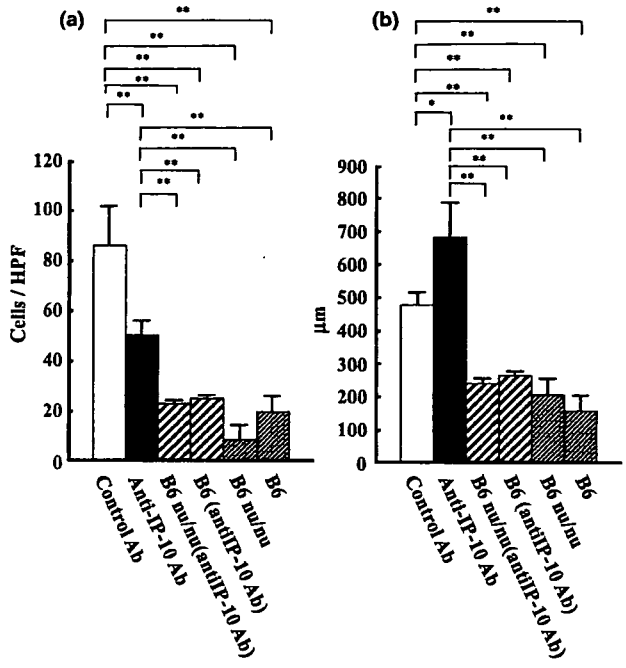

Figure 2 Effect of neutralization of interferon-γ-inducible protein 10 kDa (IP-10/CXCL10) on (a) number of infiltrating cells in the lamina propria of the colon at 3 weeks after induction of colitis and (b) crypt length of colon of mice at 3 weeks after induction of colitis. HPF, high-power field. $^*P < 0.05$; $^{**}P < 0.01$.

IP-10 neutralization reduced the number of immune cells in the colon of MAIDS colitis

Our previous immunohistochemical analyses showed that $CD4^+$ T cells and $Mac1^+$ macrophages are major populations in the colon of MAIDS colitis, with minor populations of $CD8^+$ T, and B cells.[18,21] In the present study, to determine the effect of IP-10 neutralization on the cellular components of the colon of MAIDS colitis, we analyzed the population of mucosal mononuclear cells that were isolated from the colon using a flow cytometer. In MAIDS colitis, $CD4^+$ and $CD8^+$ T cells with αβ T-cell receptors, and $Mac1^+$ cells were major populations that infiltrated the colon (Fig. 3). NK cells and granulocytes were minor populations (Fig. 3). Neutralization of IP-10 reduced the total number of inflammatory mononuclear cells infiltrating in the colon from 1.4×10^6 cells to 0.4×10^6 cells at 3 weeks after induction of the colitis. Additionally, IP-10 blockade significantly reduced the percentage

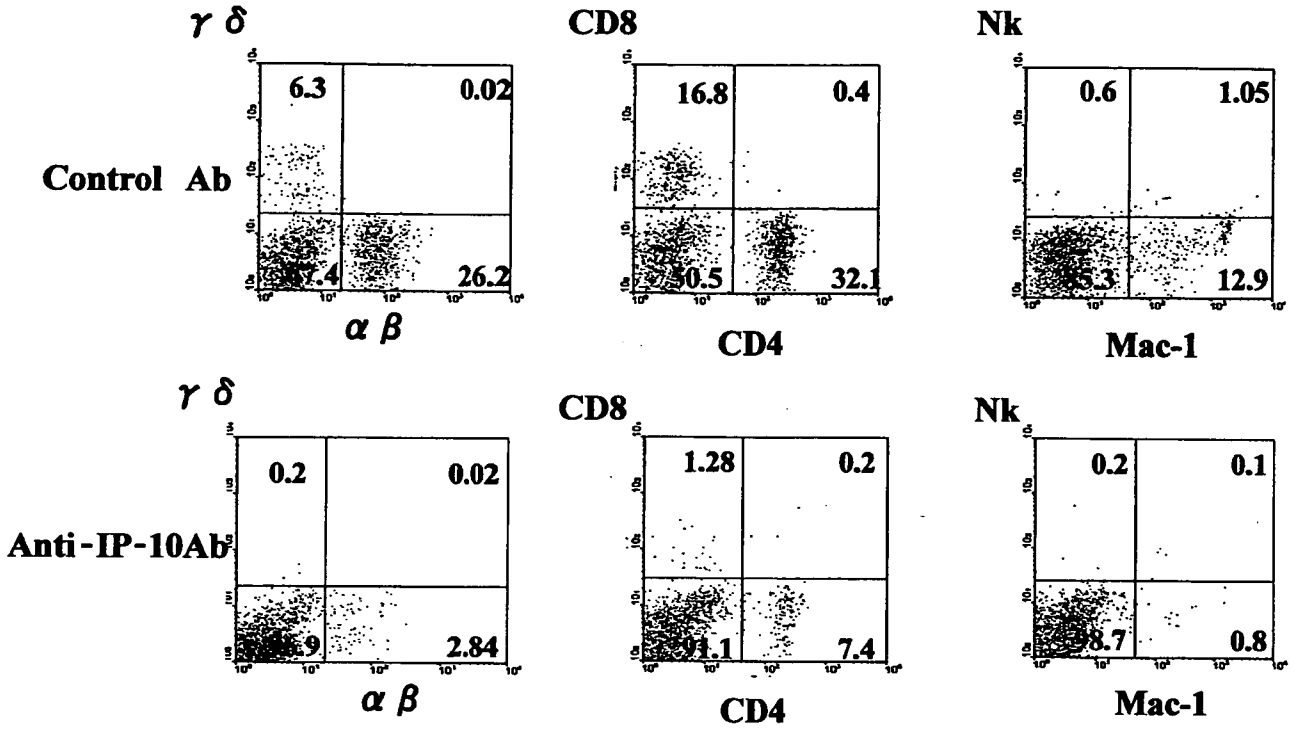

Figure 3 Neutralization of interferon-γ-inducible protein 10 kDa (IP-10/CXCL10) inhibited immune cell trafficking into the colon of murine acquired immunodeficiency syndrome (MAIDS) colitis. Two-color staining for T-cell receptor (TCR)-αβ and TCR-γδ, CD4 and CD8, and Mac1 and NK-1.1. Mononuclear cells in the colon of MAIDS mice at 3 weeks after induction of colitis were analyzed by flow cytometry; cells of mice treated with anti-IP-10 antibody were compared with those of mice treated with control antibody. Numbers in the figure represent the percentages of fluorescence-positive cells in corresponding areas. Representative results of three experiments are depicted.

of each population of $CD4^+$ and $CD8^+$ T cells possessing αβ T-cell receptors, and $Mac1^+$ cells in the colon (Fig. 3).

IP-10 neutralization increased $Ki67^+$ cells and decreased $TUNEL^+$ cells in the crypt epithelia of MAIDS colitis

We assessed the Ki67 staining to evaluate the proliferation effect of anti-IP-10 antibody treatment on colonic epithelial cells in attenuation of the colitis. In untreated B6 or B6 nude mice, $Ki67^+$ crypt epithelial cells were detected at basal one-fourth of a crypt (Fig. 4c–e). As we reported previously, crypt epithelial hyperplasia was observed in MAIDS colitis, and $Ki67^+$ cells were detected at one-third of the basal side of a crypt in the colon of MAIDS colitis with significantly increased number (Fig. 4a,e). Anti-IP-10 antibody treatment remarkably increased the number of $Ki67^+$ cells, and they were detected at a lower half of the crypt in anti-IP-10 mAb-treated mice (Fig. 4b,e).

Our previous report showed anti-apoptotic effect by IP-10 blockade on colonic epithelial cells in DSS colitis, therefore we assessed the apoptotic epithelial cells in the colons of mice with MAIDS colitis using the TUNEL method to detect DNA fragmentation *in situ*. $TUNEL^+$ apoptotic cells were observed in the epithelial cells of luminal tops of crypts in control MAIDS colitis (Fig. 5a). In anti-IP-10 antibody-treated mice, $TUNEL^+$ apoptotic epithelial cells were rarely observed (Fig. 5b).

DISCUSSION

In the present study we demonstrated that blockade of IP-10 attenuated MAIDS colitis not only by blocking cellular trafficking, but also by protecting crypt epithelial cells of the colon.

IP-10 was initially characterized as a chemoattractant for T lymphocytes, and binds to its receptor CXCR3, which is associated with Th1 immune responses.[1–4] The concept of selective mobilization of Th1 lymphocytes by IP-10 has been supported by several types of disease models[5] including multiple sclerosis,[23] rheumatoid arthritis, and inflammatory bowel disease.[11,24] Inflammatory bowel disease consists of two major forms: ulcerative colitis and Crohn's disease. Crohn's disease is suggested to be mediated by Th1-associated cytokines such as IL-23, IL-12, and IFN-γ that are overproduced by macrophages and T cells of lamina propria.

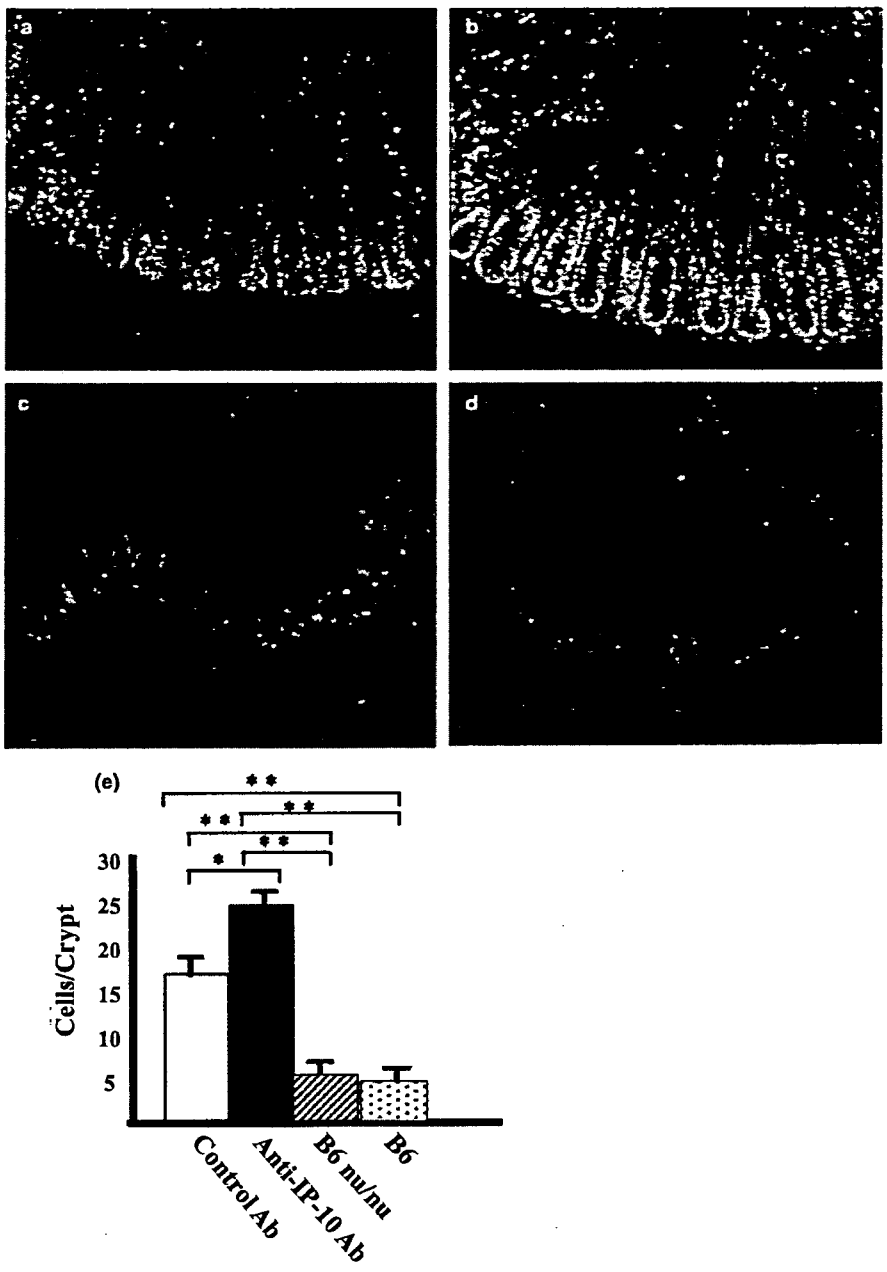

Figure 4 Neutralization of interferon-γ-inducible protein 10 kDa (IP-10/CXCL10) enhanced proliferation of crypt epithelial cells of the colon of murine acquired immunodeficiency syndrome (MAIDS) colitis. Ki67$^+$ crypt epithelial cells were detected in (**a**) control antibody-treated MAIDS colitis mouse at 3 weeks after induction of colitis; (**b**) anti-IP-10 antibody-treated MAIDS colitis mouse; (**c**) normal B6 nude mouse; and (**d**) normal B6 mouse. (**e**) The number of Ki67$^+$ crypt epithelial cells per crypt was increased in MAIDS colitis as compared with B6 and B6 nude mice. The number of cells was significantly increased by anti-IP-10 antibody treatment.

There have been developed many inflammatory bowel disease animal models. Among these, colitis observed in both IL-10-deficient mice and Rag2$^{-/-}$ mice reconstituted with CD4$^+$CD45RB^{high} T cells has been characterized as a Th1-dependent disease, mimicking Crohn's disease.[22] Scheerens *et al.* have reported increased expression of mRNA of IP-10 in Rag2$^{-/-}$ mice reconstituted with CD4$^+$CD45RB^{high} T cells, but not in IL-10-deficient mice.[24] Singh *et al.* showed that inhibition of IP-10 abrogates colitis in IL-10$^{-/-}$ mice supposedly by inhibiting the Th1 immune response.[11] They did not observe the hyperplasia of crypt epithelial cells of the colon induced by the blockade of IP-10 in the model. Thus, IP-10 neutralization is supposed to inhibit Th1 inflammatory reaction resulting in amelioration of colitis. To confirm the efficacy of the aforementioned mechanism, it is better to analyze the effect of anti-IP-10 treatment in different types of colitis models. We have established another experimental colitis model, that is, MAIDS colitis resembling ulcerative colitis.[18,21] In the present study, using this MAIDS colitis model, we also showed that IP-10 blockade significantly inhibited immune cell trafficking, leading to attenuation of the disease. Additionally we have recently reported that anti-IP-10 treatment ameliorates autoimmune-like pancreatic lesions in mice with MAIDS by blocking cellular trafficking.[25] Therefore, it is con-

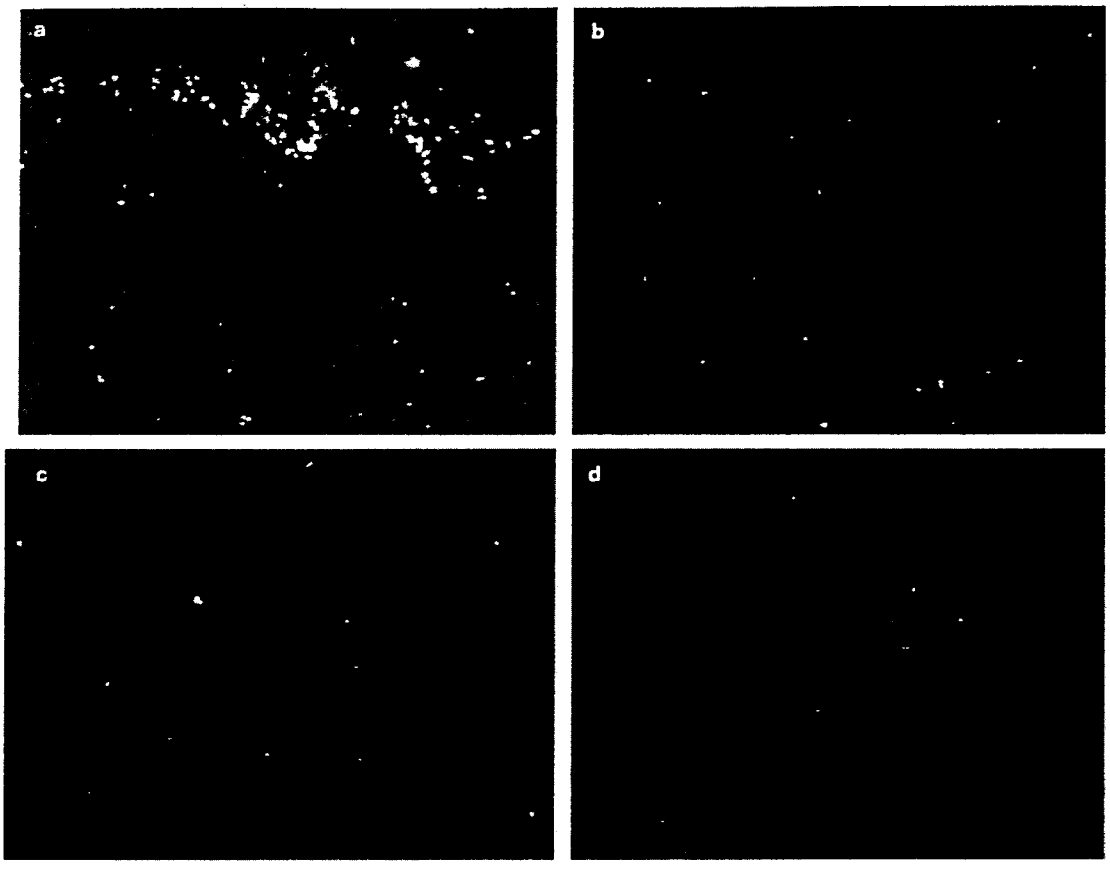

Figure 5 Anti-apoptotic death of crypt epithelial cells of colon by neutralization of interferon-γ-inducible protein 10 kDa (IP-10/CXCL10). (**a**) Terminal deoxynucleotidyl transferase-mediated dUTP nick-end labeling (TUNEL)$^+$ apoptotic cells were observed in the epithelial cells of luminal tops of crypts in murine acquired immunodeficiency syndrome (MAIDS) colitis; (**c**) TUNEL$^+$ apoptotic cells were rarely observed from B6 mice, (**d**) B6 nude mice and (**b**) mice treated with anti-IP-10 antibody.

ceivable that the main therapeutic effect of IP-10 neutralization in colitis, as well as in the other autoimmune diseases, is induced by inhibition of selective Th1 cells mobilization.

In our previous report we showed that neutralization of IP-10 protected mice from DSS-induced acute colitis by promoting crypt cell survival without altering immune cell infiltration.[10] Furthermore, recombinant IP-10 administration into normal mice directly inhibited intestinal crypt cell proliferation and migration *in vivo*.[10] Thus, we consider IP-10 a negative regulator of crypt cell proliferation and migration in the intestine. Initially DSS colitis was considered to be a T-cell-independent model because of the induction of colitis in T- and B-cell-lacking severe combined immunodeficient mice.[26] Later, however, both macrophage and T-cell responses were shown to play a pivotal role in the disease process, and the pathophysiology of DSS colitis is different from colitis observed in IL-10-deficient mice and Rag2$^{-/-}$ mice reconstituted with CD4$^+$CD45RB^{high} T cells.[22] This difference in pathophysiology of colitis might explain the different effect of IP-10 blockade on enhanced proliferation and anti-apoptosis of crypt epithelial cells or on inhibition of immune cell trafficking into the colon. As we have reported previously, both Th1 and Th2 immune responses were observed in MAIDS colitis, and hyperplasia of crypt epithelial cells is one of the characteristics of MAIDS colitis.[18,21] In the present study we demonstrated that IP-10 neutralization induced marked proliferation of crypt epithelial cells in MAIDS colitis as well as inhibition of immune cell trafficking. Neutralization of IP-10 did not show any change in the length of the crypt of the colon in B6 nude and B6 mice. In contrast, IP-10 neutralization for MAIDS colitis accelerated intestinal epithelial proliferation more significantly than untreated MAIDS colitis. These results suggest that IP-10 neutralization exerts its cell-proliferating effect more actively on the intestinal epithelial cells in inflammation, rather than on those in normal condition. We should analyze the synergistic relationship between IP-10 neutralization and cytokines and growth factors such as IFN-γ, IL-13, and IL-10, which are secreted by the immune cells recruited by IP-10, for the promotion of proliferation and anti-apoptosis of intestinal epithelial cells.

In conclusion, we have demonstrated that blockade of IP-10 ameliorated MAIDS colitis not only by blocking cellular trafficking, but also by facilitating the proliferation and anti-apoptosis of crypt epithelia of the colon. Neutralization of IP-10 could be a promising adjunctive therapy for inflammatory bowel disease.

ACKNOWLEDGMENTS

We thank Dr Xiu-Hua Yang and Mr Norio Honda for technical assistance. This work was supported by grants from the Ministry of Health, Welfare, and Labor of Japan.

REFERENCES

1 Luster AD. Chemokines: Chemotactic cytokines that mediate inflammation. *N Engl J Med* 1998; **338**: 436–45.
2 Baggiolini M. Chemokines and leukocyte traffic. *Nature* 1998; **392**: 565–8.
3 Luster AD, Ravetch JV. Biochemical characterization of a gamma interferon-inducible cytokine (IP-10). *J Exp Med* 1987; **166**: 1084–97.
4 Farber JM. Mig and IP-10: CXC chemokines that target lymphocytes. *J Leukoc Biol* 1997; **61**: 246–57.
5 Sallusto F, Lanzavecchia A, Mackay CR. Chemokines and chemokine receptors in T-cell priming and T helper 1/T helper 2-mediated responses. *Immunol Today* 1998; **19**: 568–74.
6 Uguccioni M, Gionchetti P, Robbiani DF *et al.* Increased expression of IP-10, IL-8, MCP-1, and MCP-3 in ulcerative colitis. *Am J Pathol* 1999; **155**: 331–6.
7 Narumi S, Tominaga Y, Tamaru M. Expression of IFN-inducible protein 10 in chronic hepatitis. *J Immunol* 1998; **158**: 5536–44.
8 Sorensen TL, Trebst C, Kivisakk P *et al.* Multiple sclerosis: A study of CXCL10 and CXCR3 co-localization in the inflamed central nervous system. *J Neuroimmunol* 2002; **127**: 59–68.
9 Ogawa N, Ping L, Zhenjun L, Takada Y, Sugai S. Involvement of the interferon-γ-induced T cell-attracting chemokines, interferon-γ-inducible 10-kd protein (CXCL10) and monokine induced by interferon-γ (CXCL9), in the salivary gland lesions of patients with Sjögren's syndrome. *Arthritis Rheum* 2002; **46**: 2730–41.
10 Sasaki S, Yoneyama H, Suzuki K *et al.* Blockade of CXCL10 protects mice from acute colitis and enhances crypt cell survival. *Eur J Immunol* 2002; **32**: 3197–205.
11 Singh UP, Singh S, Taub DD, Lillard JW Jr. Inhibition of IFN-γ-inducible protein-10 abrogates colitis in IL-10–/– mice. *J Immunol* 2003; **171**: 1401–6.
12 Mosier DE, Yetter RA, Morse HC III. Retroviral induction of acute lymphoproliferative disease and profound immunosuppression in adult C57BL/6 mice. *J Exp Med* 1985; **161**: 766–84.
13 Klinken SP, Fredrickson TN, Hartley JW. Evolution of B cell lineage lymphomas in mice with a retrovirus-induced immunodeficiency syndrome, MAIDS. *J Immunol* 1998; **140**: 1123–31.
14 Jolicoeur P. Murine acquired immunodeficiency syndrome (MAIDS): An animal model to study the AIDS pathogenesis. *FASEB J* 1991; **5**: 2398–405.
15 Cheung SC, Chattopadhyay SK, Hartley JW. Aberrant expression of cytokine genes in peritoneal macrophages from mice infected with LP-BM5 MuLV, a murine model of AIDS. *J Immunol* 1991; **146**: 121–7.
16 Suzuki K, Makino M, Okada Y *et al.* Exocrinopathy resembling Sjoegren's syndrome induced by a murine retrovirus. *Lab Invest* 1993; **69**: 430–35.
17 Watanabe S, Suzuki K, Kawauchi Y *et al.* Kinetic analysis of the development of pancreatic lesions in mice infected with a murine retrovirus. *Clin Immunol* 2003; **109**: 212–23.
18 Suzuki K, Narita T, Yui R *et al.* Induction of intestinal lesions in nu/nu mice induced by transfer of lymphocytes from syngeneic mice infected with murine retrovirus. *Gut* 1997; **41**: 221–8.
19 Izcue A, Coombes JL, Powrie F. Regulatory T cells suppress systemic and mucosal immune activation to control intestinal inflammation. *Immunol Rev* 2006; **212**: 256–71.
20 Fantini MC, Becker C, Tubbe I *et al.* Transforming growth factor beta induced FoxP3+ regulatory T cells suppress Th1 mediated experimental colitis. *Gut* 2006; **55**: 671–80.
21 Suriki H, Suzuki K, Baba Y *et al.* Analysis of cytokine production in the colon of nude mice with experimental colitis induced by adoptive transfer of immunocompetent cells from mice infected with a murine retrovirus. *Clin Immunol* 2000; **97**: 33–42.
22 Powrie F. T cells in inflammatory bowel disease: Protective and pathogenic role. *Immunity* 1995; **3**: 171–4.
23 Narumi S, Kaburaki T, Yoneyama H, Iwamura H, Kobayashi Y, Matsushima K. Neutralization of IFN-inducible protein10/CXCL10 exacerbates experimental autoimmune encephalomyelitis. *Eur J Immunol* 2002; **32**: 1784–91.
24 Scheerens H, Hessel E, De Waal-Malefyt R, Leach MW, Rennick D. Characterization of chemokines and chemokine receptors in two murine models of inflammatory bowel disease: IL-$10^{-/-}$ mice and Rag-$2^{-/-}$ mice reconstituted with $CD4^{+}CD45RB^{high}$ T cells. *Eur J Immunol* 2001; **31**: 1465–74.
25 Kawauchi Y, Suzuki K, Watanabe S *et al.* Role of IFN-γ-inducible protein-10 (IP-10/CXCL10) in the progression of pancreatitis-like injury in mice after murine retroviral infection. *Am J Physiol Gastrointest Liver Physiol* 2006; **291**: G345–54.
26 Dieleman LA, Ridwan BU, Tennyson GS, Beagley KW, Bucy RP, Elson CO. Dextran sulfate sodium-induced colitis occurs in severe combined immunodeficient mice. *Gastroenterology* 1994; **107**: 1643–52.

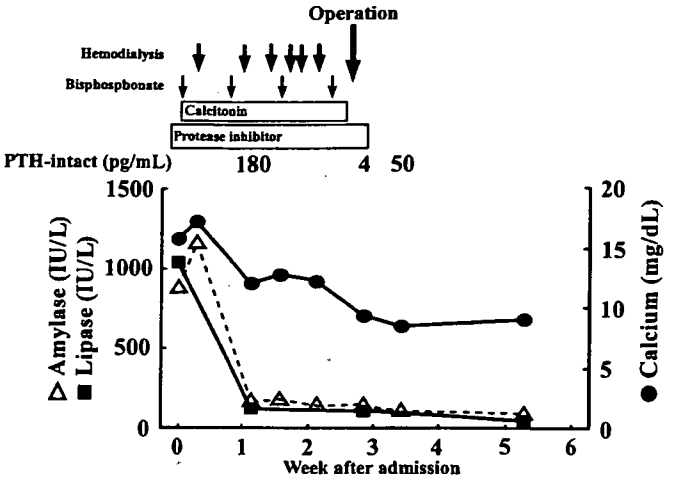

FIGURE 1. Serum levels of calcium (normal range, 8.7–10.0 mg/dL), amylase (normal range, 39–108 IU/L), lipase (normal range, ≤41 IU/L), and PTH-intact (normal range, 10–65 pg/mL) during the course of hospitalization.

Severe Acute Pancreatitis as an Initial Manifestation of Primary Hyperparathyroid Adenoma in a Pediatric Patient

To the Editor:

Acute pancreatitis (AP) is an unusual entity in childhood.[1] Here, we report a case of severe AP in a pediatric patient who was diagnosed as having primary hyperparathyroidism (pHPT) based on the presence of hypercalcemia. The patient, a 15-year-old Japanese girl, was referred to our hospital for further treatment 6 hours after developing epigastralgia. She had no history of trauma, abdominal surgery, or biliary disease. Laboratory data showed leukocytosis (24.4 × 10^9 L) and increased serum levels of amylase (890 IU/L), lipase (1045 IU/L), calcium (15.4 mg/dL), and alkaline phosphatase (1002 IU/L). Abdominal computed tomography showed acute edematous pancreatitis, with fluid collection in the peripancreas and prerenal space, but no evidence of gallbladder disease or bile duct dilatation. We administered antibiotics and a protease inhibitor for AP and saline, loop diuretic, calcitonin, and bisphosphonate for the hypercalcemia. The patient's clinical course is shown in Figure 1. On hospital day 2, the AP remained unchanged on abdominal computed tomography, and because hypercalcemia had developed (16.8 mg/dL), hemodialysis was started. Further laboratory investigation of the hypercalcemia revealed an increased serum level of parathyroid hormone (PTH)–intact (180 pg/mL; normal range, 10–65 pg/mL) and negativity for PTH-related peptide (<1.0 pmol/L). Ultrasonography and technetium Tc 99m sestamibi scintigraphy revealed a single left inferior parathyroid tumor adjacent to the thyroid lobe. Parathyroidectomy was performed, and histological examination revealed that the tumor was a parathyroid adenoma. Two days after the operation, the serum calcium and PTH-intact levels returned to normal. The patient has been followed up for 6 months without any signs of recurrence.

In children, trauma, structural anomalies, and systemic disease account for the majority of AP cases, and metabolic disorders including hypercalcemia are a rare etiology.[2] Hypercalcemia is usually caused by pHPT or malignancy, but in children, the incidence of pHPT (2–5 in 100,000) is much lower than that in adults (1 in 1000).[3] Indeed, there have been few previous reports of AP associated with pHPT in childhood.[4,5] The present case was similar to one reported by Shimizu and Kodama[5] in that severe AP was resistant to treatment, and hypercalcemia abruptly worsened. To alleviate the hypercalcemia in our patient, hemodialysis was performed repeatedly, and this rendered the AP sensitive to treatment. The relationship between AP and pHPT remains controversial, although several theories have been proposed.[6–8] In the present case, because no etiological factor for AP could be identified other than hypercalcemia due to pHPT, we suggest that there is a strong relationship between AP and pHPT. Among the forms of organ damage due to pHPT, AP is a rare but lethal one. Therefore, even in children, it is vital to take pHPT into consideration as an etiological factor in cases of severe AP with hypercalcemia.

Kiyotaka Tsuboi, MD*
Masaaki Takamura, MD, PhD*
Yuichi Sato, MD, PhD*
Hisashi Yokoyama, MD, PhD*
Manabu Takeuchi, MD, PhD*

Masato Igarashi, MD, PhD*
Daisuke Kondo, MD, PhD†
Kentaro Omori, MD, PhD†
Asa Ogawa, MD, PhD†
Aya Takeyama, MD†
Yu Koyama, MD, PhD‡
Yoichi Ajioka, MD, PhD§
Yutaka Aoyagi, MD, PhD*
Divisions of *Gastroenterology and Hepatology
†Clinical Nephrology and Rheumatology
‡Digestive and General Surgery
and §Molecular and Diagnostic Pathology
Niigata University
Graduate School of Medical and Dental Sciences
Niigata, Japan
atmc@hotmail.co.jp

REFERENCES

1. Steinberg W, Tenner S. Acute pancreatitis. *N Engl J Med.* 1994;330:1198–1210.
2. Benifla M, Weizman Z. Acute pancreatitis in childhood. *J Clin Gastroenterol.* 2003;37: 169–172.
3. Kollars J, Zarroug AE, van Heerden J, et al. Primary hyperparathyroidism in pediatric patients. *Pediatrics.* 2005;115:974–980.
4. Nieves-Rivera F, Gonzalez-Pijem L. Primary hyperparathyroidism: an unusual cause of pancreatitis in adolescence. *P R Health Sci J.* 1995;14:233–236.
5. Shimizu H, Kodama A. Severe acute pancreatitis as a first symptom of primary hyperparathyroid adenoma: a case report. *J Laryngol Otol.* 1996;110:602–603.
6. Haverback BJ, Dyce B, Bundy H, et al. Trypsin, trypsinogen and trypsin inhibitor in human pancreatic juice. *Am J Med.* 1960; 29:424–433.
7. Kuroda T, Shiohara E, Haba Y, et al. Effects of parathyroid hormone of pancreatic exocrine secretion. *Pancreas.* 1993;8: 732–737.
8. Frick TW, Mithöfer K, Fernández-del Castillo C, et al. Hypercalcemia causes acute pancreatitis by pancreatic secretory block, intracellular zymogen accumulation, and acinar cell injury. *Am J Surg.* 1995;169:167–172.

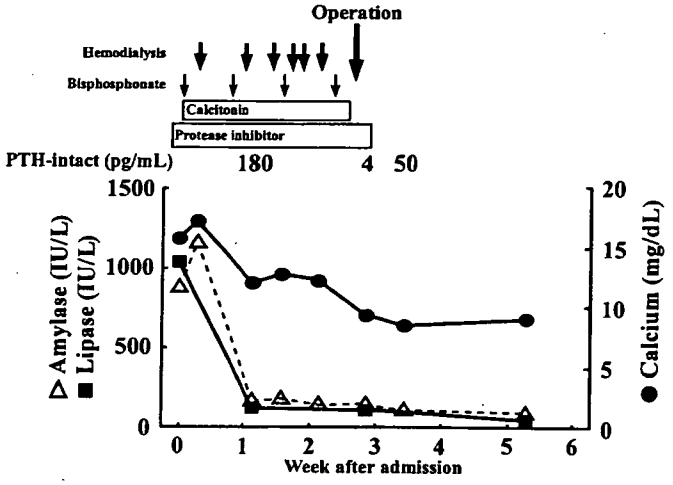

FIGURE 1. Serum levels of calcium (normal range, 8.7–10.0 mg/dL), amylase (normal range, 39–108 IU/L), lipase (normal range, ≤41 IU/L), and PTH-intact (normal range, 10–65 pg/mL) during the course of hospitalization.

Severe Acute Pancreatitis as an Initial Manifestation of Primary Hyperparathyroid Adenoma in a Pediatric Patient

To the Editor:

Acute pancreatitis (AP) is an unusual entity in childhood.[1] Here, we report a case of severe AP in a pediatric patient who was diagnosed as having primary hyperparathyroidism (pHPT) based on the presence of hypercalcemia. The patient, a 15-year-old Japanese girl, was referred to our hospital for further treatment 6 hours after developing epigastralgia. She had no history of trauma, abdominal surgery, or biliary disease. Laboratory data showed leukocytosis (24.4 × 10^9 L) and increased serum levels of amylase (890 IU/L), lipase (1045 IU/L), calcium (15.4 mg/dL), and alkaline phosphatase (1002 IU/L). Abdominal computed tomography showed acute edematous pancreatitis, with fluid collection in the peripancreas and prerenal space, but no evidence of gallbladder disease or bile duct dilatation. We administered antibiotics and a protease inhibitor for AP and saline, loop diuretic, calcitonin, and bisphosphonate for the hypercalcemia. The patient's clinical course is shown in Figure 1. On hospital day 2, the AP remained unchanged on abdominal computed tomography, and because hypercalcemia had developed (16.8 mg/dL), hemodialysis was started. Further laboratory investigation of the hypercalcemia revealed an increased serum level of parathyroid hormone (PTH)–intact (180 pg/mL; normal range, 10–65 pg/mL) and negativity for PTH-related peptide (<1.0 pmol/L). Ultrasonography and technetium Tc 99m sestamibi scintigraphy revealed a single left inferior parathyroid tumor adjacent to the thyroid lobe. Parathyroidectomy was performed, and histological examination revealed that the tumor was a parathyroid adenoma. Two days after the operation, the serum calcium and PTH-intact levels returned to normal. The patient has been followed up for 6 months without any signs of recurrence.

In children, trauma, structural anomalies, and systemic disease account for the majority of AP cases, and metabolic disorders including hypercalcemia are a rare etiology.[2] Hypercalcemia is usually caused by pHPT or malignancy, but in children, the incidence of pHPT (2–5 in 100,000) is much lower than that in adults (1 in 1000).[3] Indeed, there have been few previous reports of AP associated with pHPT in childhood.[4,5] The present case was similar to one reported by Shimizu and Kodama[5] in that severe AP was resistant to treatment, and hypercalcemia abruptly worsened. To alleviate the hypercalcemia in our patient, hemodialysis was performed repeatedly, and this rendered the AP sensitive to treatment. The relationship between AP and pHPT remains controversial, although several theories have been proposed.[6–8] In the present case, because no etiological factor for AP could be identified other than hypercalcemia due to pHPT, we suggest that there is a strong relationship between AP and pHPT. Among the forms of organ damage due to pHPT, AP is a rare but lethal one. Therefore, even in children, it is vital to take pHPT into consideration as an etiological factor in cases of severe AP with hypercalcemia.

Kiyotaka Tsuboi, MD*
Masaaki Takamura, MD, PhD*
Yuichi Sato, MD, PhD*
Hisashi Yokoyama, MD, PhD*
Manabu Takeuchi, MD, PhD*

Masato Igarashi, MD, PhD*
Daisuke Kondo, MD, PhD†
Kentaro Omori, MD, PhD†
Asa Ogawa, MD, PhD†
Aya Takeyama, MD†
Yu Koyama, MD, PhD‡
Yoichi Ajioka, MD, PhD§
Yutaka Aoyagi, MD, PhD*
Divisions of *Gastroenterology and Hepatology
†Clinical Nephrology and Rheumatology
‡Digestive and General Surgery
and §Molecular and Diagnostic Pathology
Niigata University
Graduate School of Medical and Dental Sciences
Niigata, Japan
atmc@hotmail.co.jp

REFERENCES

1. Steinberg W, Tenner S. Acute pancreatitis. *N Engl J Med.* 1994;330:1198–1210.
2. Benifla M, Weizman Z. Acute pancreatitis in childhood. *J Clin Gastroenterol.* 2003;37: 169–172.
3. Kollars J, Zarroug AE, van Heerden J, et al. Primary hyperparathyroidism in pediatric patients. *Pediatrics.* 2005;115:974–980.
4. Nieves-Rivera F, Gonzalez-Pijem L. Primary hyperparathyroidism: an unusual cause of pancreatitis in adolescence. *P R Health Sci J.* 1995;14:233–236.
5. Shimizu H, Kodama A. Severe acute pancreatitis as a first symptom of primary hyperparathyroid adenoma: a case report. *J Laryngol Otol.* 1996;110:602–603.
6. Haverback BJ, Dyce B, Bundy H, et al. Trypsin, trypsinogen and trypsin inhibitor in human pancreatic juice. *Am J Med.* 1960; 29:424–433.
7. Kuroda T, Shiohara E, Haba Y, et al. Effects of parathyroid hormone of pancreatic exocrine secretion. *Pancreas.* 1993;8: 732–737.
8. Frick TW, Mithöfer K, Fernández-del Castillo C, et al. Hypercalcemia causes acute pancreatitis by pancreatic secretory block, intracellular zymogen accumulation, and acinar cell injury. *Am J Surg.* 1995;169:167–172.

Hepatology Research 2007; 37: 477–481 doi: 10.1111/j.1872-034X.2007.00059.x

Case Report

Early upsurge in anti-HBs titer possibly caused by the immunomodulative, not by the mutagenetic effect of interferon and ribavirin

Kazuhide Yamazaki, Shogo Ohkoshi, Masaki Maruyama, Yo-hei Aoki, Masahiko Yano, So Kurita, Kenta Suzuki, Yasunobu Matsuda, Kazuhito Sugimura and Yutaka Aoyagi

Division of Gastroenterology and Hepatology, Graduate School of Medical and Dental Sciences of Niigata University, Niigata-city, Japan

A patient with chronic hepatitis B and C undergoing treatment with interferon and ribavirin showed an upsurge in hepatitis B virus surface antibody (anti-HBs) titer, accompanied by a decrease in hepatitis B virus surface antigen (HBsAg) during the early treatment phase. Simultaneously, elevation of alanine aminotransferase (ALT) was observed. Subsequently, the hepatitis B virus (HBV) DNA titer decreased and HBV e antigen (HBeAg) to anti-HBe seroconversion occurred. The anti-HBs titer gradually returned to the pretreatment level after cessation of ribavirin treatment and HBV-DNA became undetectable. We found no nucleotide mutations in HBV-DNA that could explain the sudden elevation in anti-HBs titer. The appearance of anti-HBs was considered to be a break in immune tolerance against some epitopes in HBsAg, possibly the r epitope, stimulated by interferon/ribavirin treatment. The immunomodulatory effect of ribavirin might have caused this unexpected early immune response to HBsAg that preceded seroconversion to anti-HBe.

Key words: HBV, HCV, interferon, ribavirin, subtype of HBsAg, upsurge in anti-HBs

INTRODUCTION

SEROCONVERSION OF HEPATITIS B virus surface antigen (HBsAg) to antibody (anti-HBs) is the final event of a series of dynamic serological changes that occur in the course of chronic hepatitis B virus infection.[1] However, anti-HBs is often detectable in sera with actively replicating hepatitis B virus (HBV).[2] This can be due to the presence of HBV variants that have a point mutation in the region encoding HBsAg, causing an epitope change.[2,3] In addition, anti-HBs may often be present in sera, forming a circulating immune complex with HBsAg.[4]

The major immunogenic region of HBsAg consists of a common antigenic determinant a and subtypic determinants d/y and w/r. The a determinant has a complex structure comprising amino acids spanning from 111 to 156.[5] Epitopes of d/y and w/r are determined by allelic exclusions of single amino acid substitutions at amino acids 122 and 160, respectively.[6,7] Escape mutants of the a determinant have been detected in babies given combined immunoprophylaxis with hepatitis B vaccine and hepatitis B immune globulin,[8] and also in the clinical course of chronic HBV infection.[2,3]

Currently, ribavirin is widely used as an anti-HCV drug in combination with interferon.[9] Although the precise mechanism by which it suppresses viral replication remains largely unknown, it may act either via its mutagenetic effect on viruses, eventually causing error catastrophe,[10] or via an immunomodulating function, by inducing a Th1-dominant immune response to eliminate the virus.[11]

Here, we describe a case of chronic hepatitis B and C who was treated with interferon and ribavirin and in whom treatment was unsuccessful for chronic hepatitis C. However, we observed a good outcome with respect to the HBV infection. An upsurge in anti-HBs titer and alanine aminotransferase (ALT) preceded normal HBeAg/anti-HBe seroconversion. We carried out virological analysis as well as an inhibition test on anti-HBs, and concluded that the elevation in anti-HBs titer was

Correspondence: Dr Shogo Ohkoshi, Division of Gastroenterology and Hepatology, Graduate School of Medical and Dental Sciences of Niigata University, 1-754 Asahimachi-Dori, Niigata-city 951-8122, Japan. Email: okoshi@med.niigata-u.ac.jp
Received 25 May 2006; revision 8 September 2006; accepted 22 December 2006.

probably due to a break in immune tolerance to a specific epitope in HBsAg, induced by interferon and ribavirin combination therapy.

METHODS

Patients

A 37-YEAR-OLD Japanese man had been followed for chronic hepatitis B and C in the outpatient clinic at Niigata University. He was found to be positive for HBsAg in 1988, when he was treated for acute lymphocytic leukemia. He was also found to be positive for anti-HCV in 1993. Interferon α2b (Intron A; Schering-Plough, Osaka, Japan) and ribavirin therapy was started in July 2002. Serological markers for HBV and HCV, as well as changes in serum ALT levels before and after the start of interferon and ribavirin therapy, are shown in Figure 1. A decrease in HBsAg titer (Lumipulse II; Fujirebio, Tokyo, Japan) was observed at around the 16th week after initiation of treatment, along with an upsurge in anti-HBs titer (Lumipulse II; Fujirebio, Tokyo, Japan). Interestingly, an elevation in ALT occurred simultaneously with this change in HBsAg/anti-HBs titer. Gradual decreases in both HBeAg (IMMUNIS EIA; Institute of Immunology, Tokyo, Japan) and HBV-DNA (transcription-mediated amplification [TMA]) titers followed this episode and seroconversion to anti-HBe (IMMUNIS EIA; Institute of Immunology, Tokyo, Japan) subsequently occurred. Ribavirin treatment was discontinued at the 28th week because of the limit of medical insurance for this drug at that time in Japan, and treatment with interferon only was continued for another 20 weeks. The HBsAg titer increased after cessation of ribavirin treatment and returned to the pretreatment level, and the anti-HBs titer decreased symmetrically. HCV-RNA became negative 2 months after the start of treatment, but recurred during the treatment. HBV-DNA eventually fell below the detection limit (<3.7 LGE/mL) and remained so until the time of writing (March 2007).

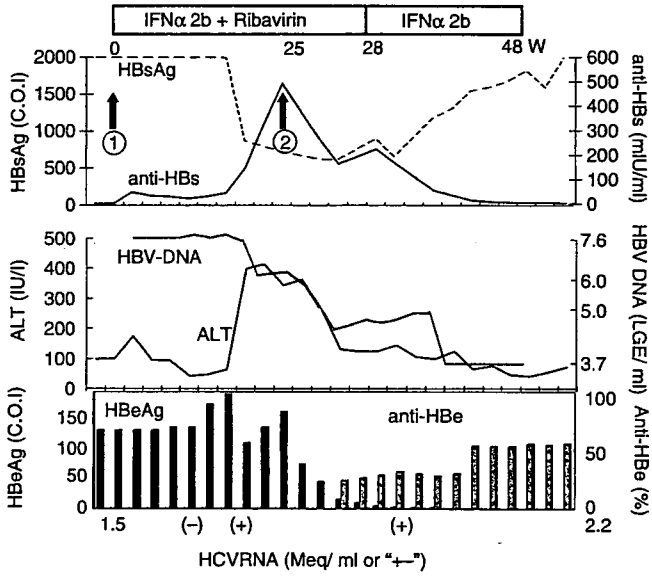

Figure 1 Clinical course and changes in virological markers in the patient before and after the start of interferon and ribavirin treatment. HBV-DNA was measured using the TMA method. The titers of HBeAg/anti-HBe were determined as a cut-off index and inhibition percent, respectively. HCV-RNAs have been indicated as titers (branched DNA probe assay) or "+, -" (Amplicor HCV qualitative test). Note that ribavirin treatment was discontinued 28 weeks after it was started. Arrows numbered 4801 and 2 show the time points for sequencing HBV-DNA.

We were interested in the mechanism by which the early upsurge in anti-HBs titer occurred during interferon and ribavirin treatment. We first tested sera from seven patients with chronic hepatitis B for anti-HBs titer obtained both before and 3 months after the initiation of interferon monotherapy, using the same assay as in this patient. None of the seven patients had an elevation in anti-HBs titer similar to that observed in the present patient (Table 1). In addition, sera obtained 6 months (patients 2 and 7) and 12 months (patient 5) after the initiation of interferon were also negative for anti-HBs.

Methods and results

We then hypothesized that mutations of the nucleotide sequence in the HBsAg region had been induced by interferon and ribavirin therapy and thus brought about amino acid changes that altered the immune reactivity of HBsAg. Using the direct sequencing method, we sequenced the complete HBV genome from sera obtained before and 25 weeks after the initiation of treatment, at which time the anti-HBs titer was at a maximum. Briefly, 14 sets of PCR primers were used to amplify the entire nucleotide sequence of HBV. KOD polymerase (Toyobo, Tokyo, Japan) was used for the PCR and the reactions were always performed in parallel with a buffer control and DNAs obtained from HBV-negative sera and other HBV-positive sera from a different carrier. The amplified fragment was purified from agarose gel and sequenced using an auto sequencer (Model 377; Applied BioSystems, Foster City, CA).

Unexpectedly, no single nucleotide mutations were observed in the HBV-DNA sequence of 3215 nucleotides

Table 1 Changes in anti-HBs titers before and 3 months after the start of interferon treatment in our patient (final row, in bold text) and seven other patients with chronic hepatitis B

	Age (years)	Sex	Diagnosis	Interferon therapy	Anti-HBs titer (mIU/ml)	
					Before	After
1	48	F	CH(B)	nIFNα	(−)0.2	(−)0.1
2	23	M	CH(B)	IFNβ	(−)0.3	(−)0.1
3	52	M	CH(B)	nIFNα	(−)0.1	(−)0.1
4	47	M	CH(B)	IFNβ	(−)0.1	(−)0.1
5	55	M	CH(B)	IFNβ	(+)178.5	(+)61.6
6	30	M	CH(B)	IFNβ	(−)0.7	(−)2.0
7	36	M	CH(B)	IFNβ	(−)0.1	(−)0.1
8	37	M	CH(B)	**IFNα+Riv**	**(−) 0.1**	**(+)29.2**

(nts) obtained from before and 25 weeks after the initiation of treatment, although there was a 79 nucleotides (2.5%) difference from the HBV genome obtained from a different HBV carrier (3215 nts, DDBJ accession number: AB288026). The identical amino acid sequence of the HBsAg region, which was subtype adr, obtained at the two time points is shown in Figure 2. We also examined the subtype of HBV in the sera before the start of the therapy by an EIA kit (IMMUNIS EIA; Institute of Immunology, Tokyo, Japan). The strong reactivity to subtypic determinants d and y was observed, while there was no reactivity to y and w. Thus, serological HBV subtype was adr, identical to that obtained by sequence analysis.

We next carried out an inhibition test against high titer anti-HBs using several subtype-specific antigens. Purified adr (Fujirebio, Tokyo, Japan), adw (HyTest, Turku, Finland) and ay that did not have w or r determinants (Biokit, Barcelona, Spain) antigens were added to the sera with high anti-HBs titers. The maximum inhibition values achieved by each antigen are shown in Figure 3. Only the adr antigen reduced the anti-HBs titer significantly, while the adw and ay antigens did not produce any effect. Thus, the main reactivity of anti-HBs could be to the r epitope of HBsAg.

DISCUSSION

WE WERE INTERESTED in the upsurge in anti-HBs titer during the early phase of interferon and ribavirin treatment in this patient. It is known that a proportion of HBsAg may be present in a patient's serum in the form of immune complex with anti-HBs.[4] Although we could not detect any anti-HBs before the start of interferon/ribavirin treatment, there is the possibility that pre-existing, undetectable anti-HBs activity increased along with the decrease in HBsAg levels, due to antiviral treatment. It was also possible that anti-HBs was present, independent of immune complex in the serum. Because we did not perform an immune complex assay, both hypotheses remain possible. However, a sudden elevation of ALT observed almost at the same time as the increase in anti-HBs (Fig. 1) appeared to result from the active effort of the cellular immune response eliminating HBsAg.

Because the main viral target of the cellular immune response is the nucleocapsid protein and HBeAg, a flare-up of hepatitis is usually seen during the process of HBeAg/anti-HBe seroconversion. However, a similar flare-up of hepatitis also may be observed during the process of immune clearance of HBsAg.[12] Although we do not know whether this flare-up of ALT was the result of immune reaction to HBeAg, or to HBsAg, at the very least it is likely to have triggered an immune response against HBV leading to the subsequent seroconversion to anti-HBe and resulting in a reduction of HBV-DNA. This immunological sequence produced a good serological prognosis for chronic hepatitis B in the present patient.

In the present case, the significant increase in anti-HBs titer that preceded the appearance of anti-HBe led us to speculate that some mutations had occurred in the HBV genome, possibly in the region encoding the antigenic determinants of HBsAg, and had induced an immune reaction against HBsAg during antiviral therapy, as has been reported elsewhere.[13] However, there were no nucleotide changes between the two time points before and after the start of the treatment. Thus, there were no amino acid changes that were responsible for the appearance of anti-HBs.

As far as the HBV-DNA sequence itself is concerned, we compared amino acid sequences with those of wild